

## X-ray diffraction study of the lattice deformation due to $^3\text{He}$ bubble formation in a tantalum tritide

R. Lässer,\* K. Bickmann, and H. Trinkaus

*Institut für Festkörperforschung, Kernforschungsanlage Jülich, D-5170 Jülich, West Germany*

(Received 24 May 1988; revised manuscript received 16 January 1989)

A previous x-ray-diffraction study of the lattice deformation developing in a tantalum tritide during the first 75 d after tritium charging is extended over about three years. The lattice spacing first increases slightly with increasing helium concentration built up upon tritium decay, reverses this tendency around 1 at. %  $^3\text{He}$ , and eventually decreases at a rate somewhat larger than the one corresponding to the decrease in the tritium concentration. Peak broadening increases almost linearly with the  $^3\text{He}$  concentration but speeds up significantly around 1 at. %  $^3\text{He}$ . Peak shifting and broadening combined with recent dilatometric measurements yield a consistent picture of the damage evolution. The main result is that in the range studied most of the tantalum self-interstitials produced on  $^3\text{He}$  bubble formation are incorporated into an evolving dislocation network.

### INTRODUCTION

Since tritium transmutes into helium, metal tritides are time-dependent ternary systems in which the increase in the helium concentration corresponds to the decrease in the tritium concentration. Whereas tritium, like the other hydrogen isotopes, is easily soluble in many metals, its daughter product  $^3\text{He}$  is, like the other inert gases, virtually insoluble in them, with solubility limits in the sub-ppm range. Therefore, helium created on tritium transmutation in metals has a strong tendency to precipitate into bubbles. At room temperature, bubble formation in tritides implies the formation of self-interstitials, which results in the evolution of a dislocation network. The primary macroscopic effect of bubble formation is swelling.<sup>1</sup> Other effects are hardening<sup>2</sup> and intergranular embrittlement.<sup>3</sup>

Recently, the lattice spacing and damage developing in monocrystalline and polycrystalline tantalum tritide samples were examined by means of x-ray<sup>4</sup> and neutron<sup>5</sup> scattering, respectively. The x-ray study performed by us covered the first 75 d after tritium charging of a monocrystalline tantalum tritide sample of composition  $\text{TaT}_{0.164-c}^3\text{He}_c$ . Subsequently, we have extended this study over a period of 1300 d. Between 300 and 600 d after tritium charging, substantial changes in the evolution of position and width of the diffraction peak occurred. After this period the observed trends stabilized and remained essentially constant up to our last measurements, so that we may now consider the study to be complete. In the present paper we report and interpret the results of the whole study and compare them with the neutron-scattering data mentioned above.

### EXPERIMENTAL PROCEDURE AND RESULTS

After proper preparation the monocrystalline tantalum sample had been charged with tritium in the Jülich-37  $\times 10^{12}$ -Bq tritium-loading facility.<sup>6</sup> The initial concentra-

tions of the hydrogen isotopes were determined to be 1.9 at. % H, 0.6 at. % D, and 16.4 at. % T.<sup>4</sup> X-ray diffraction was performed at room temperature, where such a hydride is in the pure  $\alpha$ -phase.<sup>7</sup>

The lattice spacing and damage developing in this sample was measured during about three years after T charging using the Bond method,<sup>8</sup> which permits an accurate determination of the position and width of rocking curves at Bragg positions.  $\text{Cu } K\beta$  x rays were used to study the (222) reflex of the  $\text{TaT}_{0.164-c}^3\text{He}_c$  bcc structure. Whereas the sample had been kept in the diffractometer during the first 75 d after T charging for accuracy reasons,<sup>4</sup> it was removed between the measurements during the long, subsequent observation period.

Figure 1 shows two typical (222) rocking curves plotted versus scattering angle  $\vartheta$  for 6 and 1013 d after T charging, respectively. It reveals three main changes occurring during aging: (1) a peak shift towards larger angles corresponding to a decrease of the lattice parameter, (2) a peak broadening associated with a decrease in the maximum intensity indicating the evolution of a dislocation network, and (3) an asymmetry towards higher angles indicating an asymmetry in the dislocation structure. Note that the scale of the scattering angle in Fig. 1(b) is reduced with respect to that in Fig. 1(a) by a factor of about 3. The initial peak width is mainly due to deviations of the incident x ray from monochromacy.

The results of an evaluation of a sequence of similar rocking curves as shown in Fig. 1 are presented in Fig. 2. In Fig. 2(a) the relative shift of the (222) reciprocal-lattice point with respect to its position  $G_0$  for pure Ta,  $\Delta G/G_0$  (corresponding to a relative lattice-parameter change  $\Delta a/a_0 \approx -\Delta G/G_0$ ), is plotted versus time after charging (lower abscissa) or versus atomic  $^3\text{He}$  concentration (upper abscissa). The data correspond to the mean values of the scattering angles for 80% of the maximum intensity. The solid line drawn as a guide for the eyes shows that the lattice parameter,  $\Delta a/a_0 = -\Delta G/G_0$ , first increases slightly at the previously determined rate,<sup>4</sup>  $d(\Delta a/a_0)/dc_{\text{He}} \approx 0.6 \times 10^{-2}$ , reverses this tendency

around about 1 at. %  $^3\text{He}$ , and eventually seems to decrease at a rate even larger than the one corresponding to the transmutation of T to He. The error indicated by a few error bars increases with increasing width of the rocking curves.

Figure 2(b) shows the relative broadening of the rocking curve represented by  $\delta G_{1/2}/G = \delta\vartheta_{1/2} \cos\vartheta$  versus time and He concentration before and after deconvolution, where  $\delta\vartheta_{1/2}$  is the full angular width at half the maximum of the rocking curves. Because of the increasing broadening, the deconvolution could be done more accurately than previously.<sup>4</sup> The relative broadening per unit helium concentration of the deconvoluted peaks,  $d(\delta G_{1/2}/G)_{\text{He}}/dc_{\text{He}}$ , was found to continue at the previously determined rate<sup>4</sup> of 0.21, but to accelerate around about 1 at. %  $^3\text{He}$  to a value of about 0.33. At the end of our measuring period, the broadening rate seems to decelerate somewhat again. The ratio of the widths at  $\frac{1}{2}$  and  $\frac{1}{3}$  of the maximum intensity,  $\delta G_{1/2}/\delta G_{1/3}$ , charac-

terizing the peak shape was found to stabilize around a value of 0.49 for the deconvoluted peak, a value which (different from Ref. 4) was assumed for the whole range investigated.

## DISCUSSION

For an understanding of these experimental results, we first recall the main ideas concerning the microstructural evolution associated with  $^3\text{He}$  production in tritides at room temperature. The following characteristic stages may be distinguished: (1) diffusional clustering of He in-

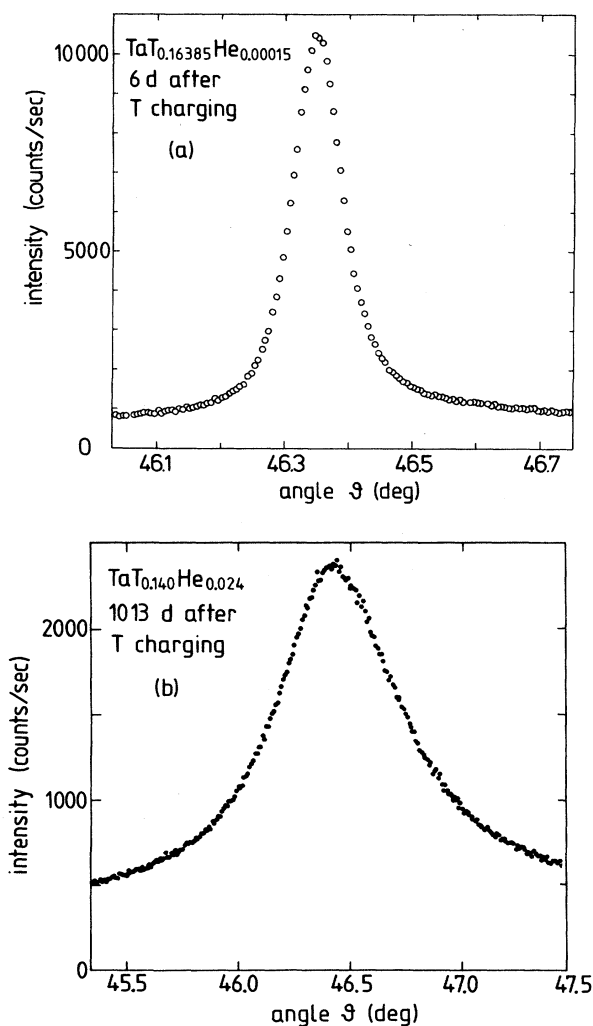


FIG. 1. Scattering intensity of a  $\text{TaT}_{0.164-c}^3\text{He}_c$  single crystal vs scattering angle  $\vartheta$  around the (222) reflex: (a) 6 d, and (b) 1013 d after T charging.

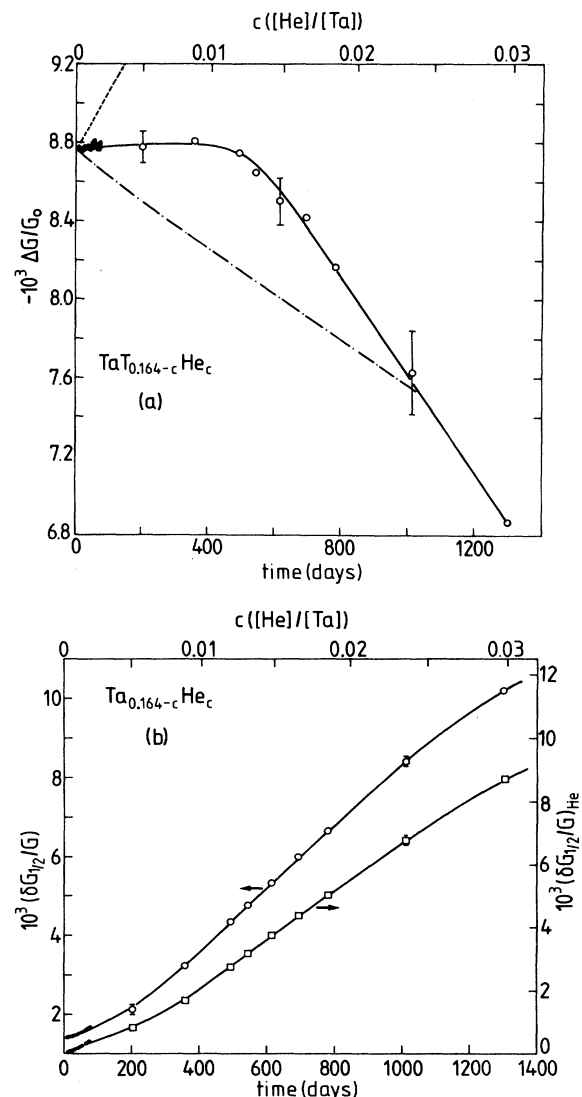


FIG. 2. (a) Relative shift and (b) broadening of the (222) rocking curve vs time (lower abscissa) or  $^3\text{He}$  concentration (upper abscissa) for a  $\text{TaT}_{0.164-c}^3\text{He}_c$  single crystal at 30.0°C. Solid symbols, previous study Ref. 4; open symbols, this study. Dashed and dashed-dotted lines in (a) for complete SIA conservation and annihilation, respectively. In (b) the full width at half the maximum is used (left ordinate, as measured; right ordinate, deconvoluted).

terstitial atoms, (2) spontaneous formation of Frenkel pairs when the number of He interstitial atoms in a cluster exceeds a certain value,<sup>9</sup> (3) formation of dislocation loops from self-interstitial atoms (SIA's) bound to the resulting He-vacancy clusters or bubbles, respectively, and their punching out from the latter,<sup>10</sup> (4) formation of a network of dislocations or dislocation dipoles from dislocation loops,<sup>11</sup> and possibly (5) the formation of subgrain boundaries by dislocation rearrangement.<sup>11</sup>

The primary macroscopic effect of self-interstitial-atom and bubble formation is swelling. Moreover, these processes result in lattice expansion and distortion fields manifesting themselves in shifts of the Bragg peaks (shrinkage of the reciprocal lattice) and diffuse scattering around them, respectively, provided the SIA's reside in the lattice as single point defects or within isolated clusters.<sup>12</sup> If SIA's are incorporated into an existing dislocation network, they may cause an increase in the dislocation density manifesting itself in a broadening of the generally unshifted peaks.<sup>12</sup> If the volume fraction of the bubbles containing gas under high pressure is substantial, they may contribute to peak broadening, too, without contributing significantly to peak shifting.<sup>12</sup> But even in such cases the maxima of the then asymmetric peaks may be shifted if the distribution of defects, particularly of tritium, becomes essentially inhomogeneous and/or if dislocation dipoles of one type are predominantly formed (see below).

Ignoring the latter possibilities for the moment, we employ the method of Simmons and Balluffi<sup>13</sup> to estimate the fraction of SIA's residing in the lattice versus that incorporated into the dislocation network, respectively. According to this, the total excess vacancy concentration resulting from the transfer of SIA's from bubbles to dislocations, grain boundaries, or surfaces is defined by the difference in the relative expansions of the sample and the crystal lattice, in reference to the defect-free state,  $\Delta L/L_0$  and  $\Delta a/a_0$ ,

$$c_V - c_I = 3(\Delta L/L_0 - \Delta a/a_0). \quad (1)$$

Here,  $c_V$  is the total concentration of vacancies contained in He bubbles and  $c_I$  is the total concentration of single SIA's and SIA's contained in isolated clusters.

According to Eq. (1),  $\Delta a/a_0 = \Delta L/L_0$  for complete SIA conservation,  $c_I = c_V$ . On the other hand,  $\Delta a/a_0 = c_T \Delta v_T / 3\Omega$  for complete SIA annihilation, where  $c_T$  is the instantaneous T concentration and  $\Delta v_T / \Omega$  is the volume change per T atom and Ta atomic volume  $\Omega$ . In Fig. 2(a) the upper (dashed) and lower (dashed-dotted) lines represent these two extreme cases when, for  $\Delta a/a_0$ , and initial value of  $\Delta a/a_0 = \Delta L/L_0 = 8.75 \times 10^{-3}$ ,  $3d(\Delta L/L_0)/dc_{He} = 0.37$  (Ref. 1), a T decay constant of  $0.178 \times 10^{-8} \text{ s}^{-1}$ , and  $\Delta v_T / \Omega = 0.138$  (Ref. 4) is assumed.

All our experimental points for  $\Delta a/a_0$  lie between these extreme cases. Even at our first measuring date, 6 d after T charging, when less than  $2 \times 10^{-4} \text{ } ^3\text{He}$  had been produced,  $\Delta a/a_0$  is clearly smaller than  $\Delta L/L_0$ , indicating that a significant fraction of the simultaneously produced SIA's had been already incorporated into the dislo-

cation network. Using  $c_V = 0.53c_{He}$  from Ref. 1, we find that for  $c_{He} < 0.01$ , where  $d(\Delta a/a_0)/dc_{He} \approx 0.6 \times 10^{-2}$ , about 70% of the SIA's produced upon bubble formation are incorporated into the dislocation network. Above 1 at. %  $^3\text{He}$  this fraction increases and seems to reach 100% at the end of our measuring period, thereby increasing the dislocation density continuously.

In this context the increasing asymmetry of the rocking curve demands some attention. Actually, it is the first moment of the peak rather than the position of its maximum which defines the average lattice spacing. In the late stage of our experiment, the estimated first moments yield values for  $\Delta a/a_0$  significantly below those corresponding to the decrease in the average T concentration due to T transmutation into  $^3\text{He}$ . This indicates an additional reduction of the T concentration in the matrix possibly resulting from T trapping by the evolving dislocation network.

Information on the dislocation system is provided by the width and the shape of the rocking curve, which represent a measure for the dislocation density and an indicator for the character of the dislocation distribution, respectively. Three main types of dislocation distributions must be considered: "restrictedly" random distribution of single dislocations,<sup>14</sup> random distributions of narrow dislocation dipoles of interstitial type with dipole separations of some Burgers vectors, and dislocations in subgrain boundaries.

Misorientations associated with the latter type of distribution could indeed account for the broadening of our rocking curves, but not for a significant broadening of Debye-Scherrer profiles of equivalent polycrystalline materials, as has been observed in neutron scattering.<sup>6</sup> We conclude that within the aging periods considered so far, dislocations of one sign do not predominantly accumulate in subboundaries.

Random distributions of narrow dislocation dipoles of interstitial type which could form from interstitial dislocation loops could account for the broadening of rocking curves as well as Debye-Scherrer profiles, but would result in a peak shift corresponding to that of an equivalent distribution of isolated interstitial-type dislocation loops for which  $\Delta a/a_0 = \Delta L/L_0$ , in disagreement with our observations. Therefore, this type of distribution can be ruled out, too. The asymmetry of the rocking curves (more intensity at the high-angle side) has, however, the direction as expected for interstitial-type dislocation loops,<sup>15</sup> indicating at least some preference of extended interstitial-type dislocation dipoles in an otherwise (restrictedly) random distribution of single dislocations.

For such a dislocation system the relative peak width,  $\delta G_{1/2}/G$ , scales as  $b\sqrt{\rho}$ , where  $b$  is the magnitude of the Burgers vector and  $\rho$  is the dislocation density.<sup>14</sup> The numerical factor depends upon the characteristics of the individual dislocations and their spatial distribution as well as on the scattering geometry. Since, in our case, the dislocations are expected to originate in SIA condensation, we assume them to be of pure edge character. The main characteristics of their distribution manifest themselves in the peak shape. Our low value of 0.49 for  $\delta G_{1/2}/\delta G_{1/5}$  indicates that the screening length in the

dislocation distribution is of the order of the dislocation distance. For this case, Wilkens's theory of peak broadening by "restrictedly" random distributions of dislocations<sup>14</sup> is doubtful. We have, therefore, extended the theory<sup>11</sup> to more general dislocation distributions than considered by Wilkens. For the broadening of our (222) rocking curves we have found

$$(\delta G_{1/2}/G)_D = \delta \vartheta_{1/2} \cos \vartheta \approx K b \sqrt{\rho}, \quad (2)$$

where  $K = 0.2$  (somewhat smaller than in Ref. 4) for  $\delta G_{1/2}/\delta G_{1/5} = 0.49$ . Assuming as Burgers vectors those of perfect dislocations in the bcc structure,  $\mathbf{b} = (1, 1, 1)a/2$  (here, Ref. 4 contains a typographical error) and  $(\delta G_{1/2}/G)_D = (\delta G_{1/2}/G)_{\text{He}}$ , we find  $d\sqrt{\rho}/dc_{\text{He}} \approx 0.4 \times 10^{10}$  and  $0.6 \times 10^{10} \text{ m}^{-1}$  for the early and late stages, respectively. At the end of our measuring period, 1301 d after T charging,  $\rho \approx 2 \times 10^{16} \text{ m}^{-2}$ .

A contribution of bubbles containing gas under pressures  $p$  of more than 5 GPa (Ref. 1) to peak broadening must be considered when their volume fraction  $f$  becomes substantial. Applying the relevant formulas in Ref. 12, we derive

$$(\delta G_{1/2}/G)_B \approx \frac{2}{3} \frac{p}{\mu} f \approx \frac{1}{3} \frac{p}{\mu} c_{\text{He}}, \quad (3)$$

where  $\mu \approx 70$  GPa is the shear modulus of the matrix. Accordingly, the peak broadening by bubbles is linear in the  $^3\text{He}$  concentration, in agreement with our measurements, but the magnitude of the broadening rate is considerably lower. For pressures between 5 and 10 GPa the bubbles amount to about 10–20 % of the broadening. Neglecting their contribution, we overestimate the dislocation density by only about 20–50 %.

In a previous paper<sup>4</sup> we had concluded that T trapping by dislocations was negligible during the first 75 d after T charging studied then. This is no longer true at the end of our present measuring period. After 1301 d of aging, dense tritidelike Cottrell clouds of 2 nm in diameter along the then-formed dislocations<sup>16</sup> of a density of  $2 \times 10^{16} \text{ m}^{-2}$  would contain about 40% of the remaining T. This supports our previously mentioned suspicion that in the late stage the reduction of the T concentration within the matrix could be significantly greater than by T transmutation into  $^3\text{He}$  alone. Contributions of T Cottrell clouds to peak broadening could then also become important.

The concentration of SIA's required to generate a dislocation system of an observed density  $\rho$  may be estimated in the following way.<sup>11</sup> Since the dislocation system consists of about equal numbers of dislocations of one and the opposite sign, it may be considered to be built up by interstitial-type dislocation dipoles ordered according to the separation of their constituents (a square lattice of edge dislocations was considered in Ref. 4). The concentration of SIA's contained in such a dipole system of density  $\rho/2$  is

$$c_V - c_I = bD\rho/2 \approx 2.5D\sqrt{\rho}(\delta G_{1/2}/G)_D, \quad (4)$$

where  $D$  is the average dislocation dipole separation. Information on  $D\sqrt{\rho}$  is provided by the shape of our rock-

ing curves.<sup>11,14</sup> From  $\delta G_{1/2}/\delta G_{1/5} = 0.49$  we deduce  $D\sqrt{\rho} \approx 0.75$ . Using this and  $(\delta G_{1/2}/G)_D = (\delta G_{1/2}/G)_{\text{He}}$ , and, in addition,  $c_V \approx 0.53c_{\text{He}}$  from Ref. 1, we find  $c_V - c_I \approx 0.74c_V$  and  $1.17c_V$ , for the beginning and end of our measuring period, respectively. In view of the limited accuracy of our analysis, this represents an excellent confirmation of our above conclusion that in the early stage a significant fraction and in the late stage practically all the generated SIA's are used to build up the dislocation system. Hence, we may say that peak shifting and broadening yield a consistent picture of the damage evolution.

Finally, we briefly comment on the neutron-scattering study of polycrystalline TaT samples mentioned above.<sup>5</sup> There is some qualitative agreement with our study concerning the sign of the lattice-parameter change for  $c_{\text{He}} < 1$  at. % and significant peak broadening due to lattice damage even in the early stage. But there is severe quantitative disagreement concerning these effects and even qualitative disagreement concerning their temporal evolution. The neutron-scattering data yielded, different from our result,  $\Delta a/a_0 \approx \Delta L/L_0$ , which would indicate that most of the SIA's produced upon bubble formation reside in the lattice as single SIA's or within isolated SIA clusters. Such a defect structure would result in diffuse scattering rather than peak broadening. The Debye-Scherrer lines measured in neutron scattering were, however, significantly broadened, even more than in our study, indicating the evolution of a dislocation network. It is unclear how this could arise from SIA clusters staying isolated in the lattice.

One possibility of resolving this inconsistency would be to assume the formation of narrow dislocation dipoles, which we have ruled out, however, for our case. The disagreement between the two studies could be due to differences in the methods: examination of a near-surface region of a monocrystal in our case and of the bulk of polycrystals in the other. We think, however, that the neutron-scattering data are not sufficiently accurate to yield a consistent picture of the underlying lattice damage as our present study does.

## CONCLUSIONS

Our experimental results and their interpretation may be summarized as follows.

In the early stage of aging, up to about 1 at. %  $^3\text{He}$ , the decrease in the lattice parameter resulting from T decay is slightly overcompensated by the increase associated with the formation of isolated SIA's and/or SIA clusters. For this stage, the analysis of peak shifting and broadening combined with recent dilatometric measurements yield that about 70% of the SIA's produced upon bubble formation are incorporated into an evolving dislocation network.

Above 1 at. %  $^3\text{He}$  a change in the time dependence of the position and width of the rocking curves is observed. The slight lattice-parameter increase is reversed into a decrease, which eventually becomes even faster than that according to the T decay. At about the same  $^3\text{He}$  con-

centration, the broadening of the rocking curves accelerates. Both effects can be explained by assuming that in this stage practically all of the SIA's produced are built into the dislocation network. Above 2 at. %  $^3\text{He}$  the analysis of peak broadening yields dislocation densi-

ties above  $10^{16} \text{ m}^{-2}$ . Removal of T from the matrix to the evolving dislocation system explains why in this stage the lattice-parameter decrease is in excess of the rate expected from the T decay.

---

\*Present address: JET Joint Undertaking, Abingdon, Oxfordshire OX14 3EA, United Kingdom.

<sup>1</sup>T. Schober, R. Lässer, J. Golczewski, C. Dieker, and H. Trinkaus, *Phys. Rev. B* **31**, 7109 (1985).

<sup>2</sup>T. Schober, C. Dieker, and H. Trinkaus, *J. Appl. Phys.* **65**, 117 (1989).

<sup>3</sup>M. I. Baskes, *Mater. Res. Bull.* **11**, 14 (1986).

<sup>4</sup>R. Lässer, K. Bickmann, H. Trinkaus, and H. Wenzl, *Phys. Rev. B* **34**, 4364 (1986).

<sup>5</sup>O. Blaschko, G. Ernst, P. Fratzl, G. Krexner, and P. Weinzierl, *Phys. Rev. B* **34**, 4985 (1986).

<sup>6</sup>R. Lässer, K. H. Klatt, P. Mecking, and H. Wenzl, Kernforschungsanlage Jülich Report No. JÜL-1800, 1982, ISSN 0336-0855 (unpublished); R. Lässer and K. H. Klatt, *Phys.*

*Rev. B* **28**, 748 (1983).

<sup>7</sup>R. Lässer, *J. Nucl. Mater.* **155-157**, 766 (1988).

<sup>8</sup>W. L. Bond, *Acta Crystallogr.* **13**, 814 (1960).

<sup>9</sup>W. D. Wilson, C. L. Bisson, and M. I. Baskes, *Phys. Rev. B* **24**, 5616 (1981).

<sup>10</sup>H. Trinkaus and W. G. Wolfer, *J. Nucl. Mater.* **122&123**, 552 (1984); W. G. Wolfer, *Philos. Mag. A* **58**, 285 (1988).

<sup>11</sup>H. Trinkaus (unpublished).

<sup>12</sup>M. A. Krivoglaz, *Theory of X-Ray and Thermal Neutron Scattering by Real Crystals* (Plenum, New York, 1969).

<sup>13</sup>R. O. Simmons and R. W. Balluffi, *Phys. Rev.* **117**, 52 (1960).

<sup>14</sup>M. Wilkens, *Phys. Status Solidi A* **2**, 359 (1970).

<sup>15</sup>H. Trinkaus, *Phys. Status Solidi B* **54**, 209 (1972).

<sup>16</sup>R. Kirchheim, *Acta Metall.* **30**, 1069 (1982).